Chalcogenide Letters Vol. 17, No. 12, December 2020, p. 615 - 621

FACILE SYNTHESIS AND GROWTH MECHANISM OF TRIGONAL SELENIUM NANOWRIES

W. B. LEI, W. Q. XU, R. J. Qi*, R. HUANG
Department of Electronic Engineering East China Normal University No. 500, Dongchuan Rd., Shanghai, 200241, P. R. China

Trigonal selenium (t-Se) nanowires were fabricated via a facile solution-phase approach at room temperature. Time-dependent experiments were designed to explore the mechanism of the transition of a-Se to t-Se both in solution and in solid phases. It was found that the extended spiral chains of selenium atoms in the trigonal phase provided a natural template to define and guide the growth direction. The transition of a-Se to t-Se nanowire can happen not only in a solid-solution-solid process, but also in a solid to solid process. The synthesis method will provide a new approach for research on its performance.

(Received August 11, 2020; Accepted December 10, 2020)

Keywords: Selenium nanowires, Trigonal phase, Solid-solution-solid

1. Introduction

During these years, one-dimensional (1D) nanomaterials such as nanorods[1], nanowires[2], and nanotubes[3], have received a great deal of attention. .Up to now, there are many ways to synthesize nanomaterials, including template assisted electrodeposition technique[4,5], template-free solution method[6], microwave polyol method[7], solvothermal synthesis[8], hydrothermal synthesis[9], sonochemical approach[10], solution-phase route[11], and a wet chemical method[12]. Among all these methods, the solution-phase route seems more promising for producing 1D nanomaterial in terms of low cost, process simplicity and high-yield [3].

Se, an important element semiconductor, has superior physical and chemical properties. Except its photoconductivity (0.8×10^{4}S/cm), which has been exploited for xerography, rectification, and solid-state light sensing applications, trigonal Se is also a well-known piezoelectric material with d_{11}=6. 5×10^{-11} C/N (~30 times larger than that of quartz)[13] and band gaps of 1.85 eV (indirect) and 1.95 eV (direct)[14]. With superior physical and chemical properties, selenium is used in photocells, photographic exposure meters, solar cells, semiconductor rectifiers and xerographic copying machines, and used as a dehydrogenating agent and as a catalyst in certain fat hardening and other processes[15]. The growth mechanism of t-Se nanowires have been extensively explored in previous studies. Gates et al[10] have synthesized Se nanowires by a sonochemical approach, which needed a long aging time for t-Se nanowires formation. Steichen M et al[16] have demonstrated the synthesis of t-Se nanorods by template-free electrodeposition at

* Corresponding author: rjqi@ee.ecnu.edu.cn

high temperature, and found that the growth process of t-Se nanorods was in agreement with a liquid-solid phase transformation of a-Se to t-Se. But this method involved high reaction temperature and some special expensive instruments as well as complicated synthesis process. So far as we know, reports on the rapid and facile synthesis of t-Se nanowires by solution-phase method at room temperature have not been presented.

In this paper, we report the rapid and facile synthesis of t-Se nanowires by solution-phase method at room temperature. Time-dependent experiments were designed to explore the mechanism of the transition of a-Se to t-Se both in solution and in solid phases. The t-Se nanowires were characterized by XRD, SEM, TEM, Raman. The results of time-dependent experiments showed that the growth of t-Se nanowires agreed with solid-solution-solid growth mechanism.

2. Experimental

Selenourea (CH_4N_2Se) was bought from Sigma–Aldrich, used without further purification. In a simple process of preparing t-Se nanowires, 5.9 mg CH_4N_2Se was dissolved in 2 mL deionized water in a 50mL centrifugal tube. The centrifugal tube containing the solution was kept vigorous stirring. After 5 minutes, the solution gradually turned brick-red at room temperature, indicating the formation of amorphous Se colloids (a-Se). Part of brick-red precipitate was collected by centrifugation and washed with deionized water and absolute ethanol for three times, respectively. The residual brick-red solution was sealed and stored in darkness at room temperature for 2h. Then the as-prepared black powders were collected and washed. The morphology of the samples was characterized by scanning electron microscope (SEM: Gemini SEM450, ZEISS, Germany) equipped with an X-ray energy dispersive spectroscope analyzer (EDS: Aztec live, Oxford Instruments, UK). The crystal structure of the product was identified by X ray diffraction (XRD: D8 Discover, Bruker, Germany). Detailed microstructure was investigated by transmission electron microscopy (TEM, HRTEM: JEM-2100F, JEOL, Japan), working at an accelerating voltage of 200 kV equipped with an X-ray energy dispersive spectrometer (EDS: X-Max 80T, Oxford, UK) for chemical composition analyses. The Raman analysis (RM1000-Invia, Renishaw, UK) was performed from 100 to 600 cm^{-1} at room temperature.

3. Results and discussion

3.1. Characterization of the as-prepared t-Se nanowires

The crystal structure of the as-prepared sample and the commercial trigonal selemium powders were characterized by X-ray diffraction and Raman spectroscopy. Fig. 1(a) shows the typical XRD pattern of the as-prepared sample (red). All the diffraction peaks of this sample could be indexed as trigonal selenium with lattice parameters of a = 4.369 Å and c = 4.944 Å, which were consistent with the reported data (JCPDS card No. 06-0362, a = 4.3662 Å and c = 4.9536 Å). Compared with XRD pattern of the commercial trigonal selenium powder (blue), it can be seen that the intensity of (100) peak of the as-prepared sample (red) was enhanced a lot, which implied that the [001] was the main growth direction of this sample. Fig. 1(b) was the Raman spectra of the

as-prepared sample (purple) and the commercial Se powders (orange). For the commercial Se powders, it was seen that only one faint peak at 235 cm^{-1} was detected in the Raman spectra. But for the as-prepared sample, the resonance peak of the characteristic signature of t-Se at 235 cm^{-1} was much higher, implying that the as-prepared sample might having a special growth orientation which is consistent with the XRD results. The resonance peaks at 141cm^{-1} corresponds to the transverse optical phone mode (E mode). Another two peaks at 433 cm^{-1} and 454 cm^{-1} can be attributed to the second-order spectra of t-Se. Furthermore, no peaks of amorphous selenium at 256 cm^{-1} and 264 cm^{-1} appeared in the Raman spectrum of the as-prepared sample, which indicated that the amorphous selenium completely transformed into trigonal selenium [17].

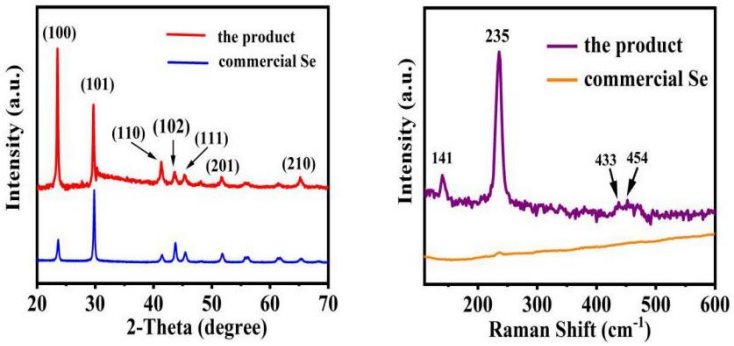

a) *b)*

Fig. 1. (a) XRD patterns of the as-prepared sample and the commercial Se powders; (b) Raman spectra of the as-prepared sample and the commercial Se powders.

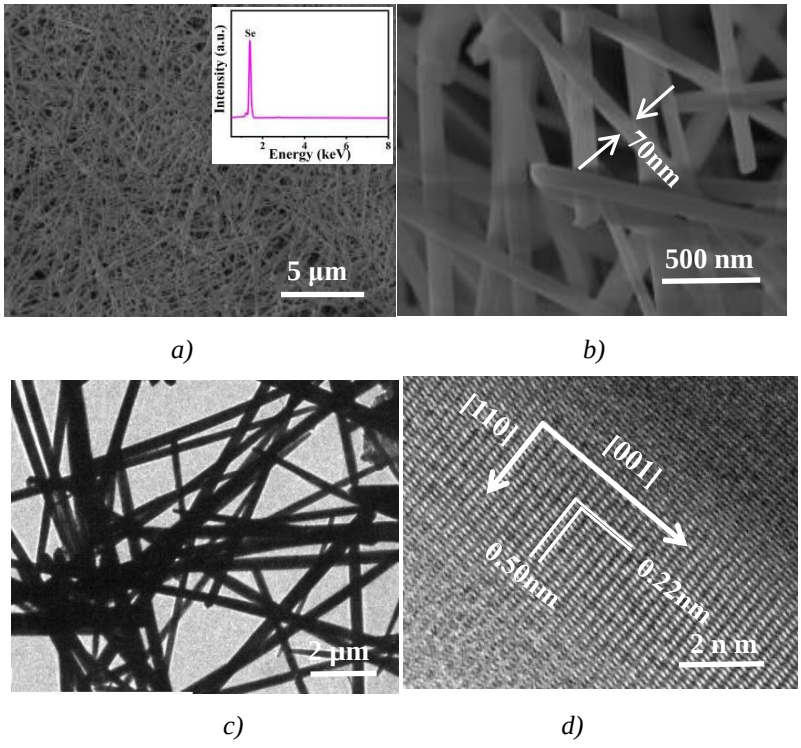

a) *b)*

c) *d)*

Fig. 2. (a) SEM image of t-Se nanowires. Inset was the EDS spectrum of t-Se nanowires; (b) Zoom in SEM image of Fig. 2 (a); (c) TEM image of t-Se nanowires. (d) HRTEM image revealed the growth of Se nanowire was along [001].

To further investigate the morphology of the sample, SEM and TEM analyses were performed. Fig. 2 is SEM and TEM images of t-Se nanowires prepared in 2 mL water containing 5.9 mg CH_4N_2Se with 2h aging time at room temperature in darkness. As shown in Fig. 2(a), it can be seen that the as-prepared sample was t-Se nanowires with lengthes up to several tens of micrometers. No obvious Se nanoparticles appeared on the t-Se nanowires, which implied that the Se nanoparticles had been completely transformed into t-Se nanowires. Inset EDS spectrum in fig. 2(a) revealed that the as-prepared product was only consisted of elemental selenium. Zoom in SEM image in Fig. 2(b) showed that the diameter of as-prepared nanowires was about 70-80 nm. TEM and HRTEM images in Fig. 2(c) and (d) displayed that the interplanar spacing of the crystal planes perpendicular to and parallel to the long axis direction of the t-Se nanowires were about 0.50 nm and 0.22 nm, corresponding to (001) planes and (110) planes of t-Se, respectively. In addition, the continuous fringes revealed that the nanowires, with few defect, had a very superior crystal quality.

3.2. The growth mechanism of t-Se nanowires

3.2.1. The transformation of a-Se to t-Se nanowires

To explore the growth mechanism of t-Se nanowires in solution, time-dependent experiments at room temperature were designed.

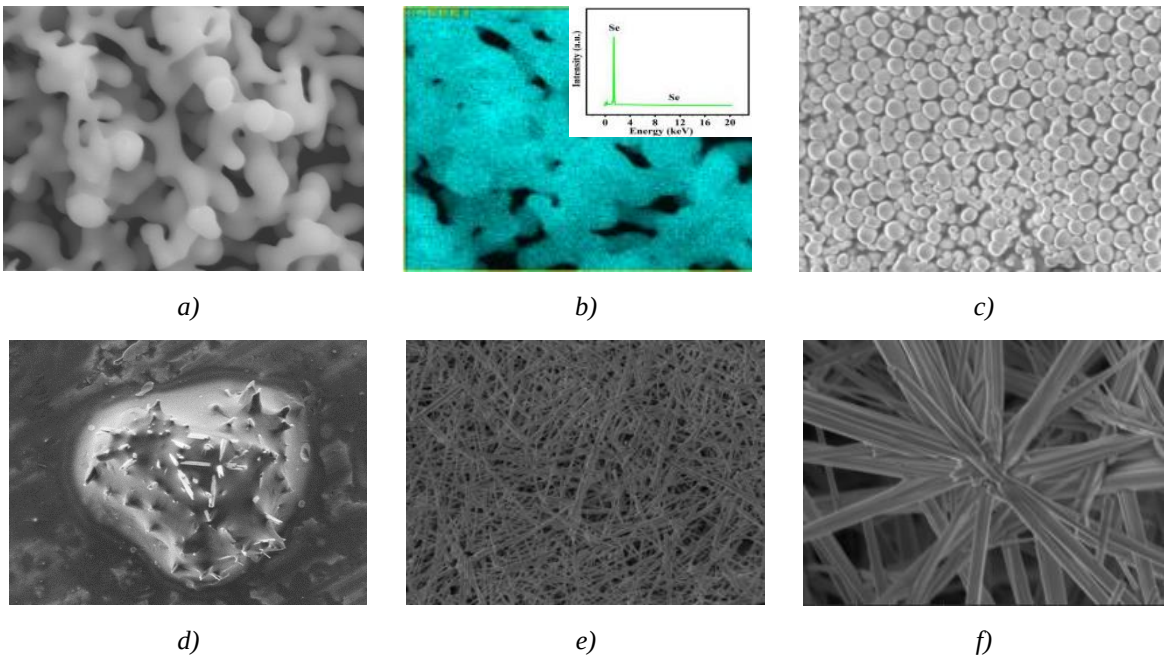

Fig. 3 SEM images of the as-prepared samples in H_2O at room temperature for different aging time; (a) and (b) 2 min, inset is the EDS spectrum of a-Se; (c) 5 min; (d) 20 min; (e) and (f) 3 h.

SEM images in Fig. 3(a) showed that amorphous Se colloids (a-Se) began to form after 2 min reaction. From the EDS mapping in Fig 3b and the inset EDS spectrum, it can be seen that the amorphous colloids were only consisted of elemental selenium. SEM image in Fig. 3(c) revealed that after 5 min aging, the network-like Se colloids turned to be spherical. As shown in Fig. 3d, it can be seen that a small quantity of t-Se nanowires seeds began to appear on the surface of a-Se

colloids after 20 min. After the aging time was extended to 3h or above, Se colloids disappeared gradually and a large number of t-Se nanowires formed (Fig. 3e). The zoom in SEM image in Fig. 3f showed that a-Se colloids were consumed completely.

3.3.2 The solid-solid transformation of a-Se to t-Se nanowires

To investigate the solid to solid transition process of Se colloids, a series of time dependent experiments were carried out at 100℃ in a vacuum oven. Fig. 4 is SEM images of samples taken at different aging time. Fig. 4a is SEM image of spherical Se colloids obtained by dissolving 5.9 mg CH_4N_2Se in 2 mL water and keeping stirring for 5 minutes at room temperature. After 1h aging, some t-Se seeds formed at the surface of Se colloids as shown in Fig. 4b. After extending the aging time to 2h (Fig. 4c), both the numbers and average lengths of selenium nanowires were clearly increased. When the aging time was increased to 6 h or above, longer Se nanowires (Fig. 4d) formed. Inset SEM image in Fig. 4d showed that spherical Se colloids were completely consume.

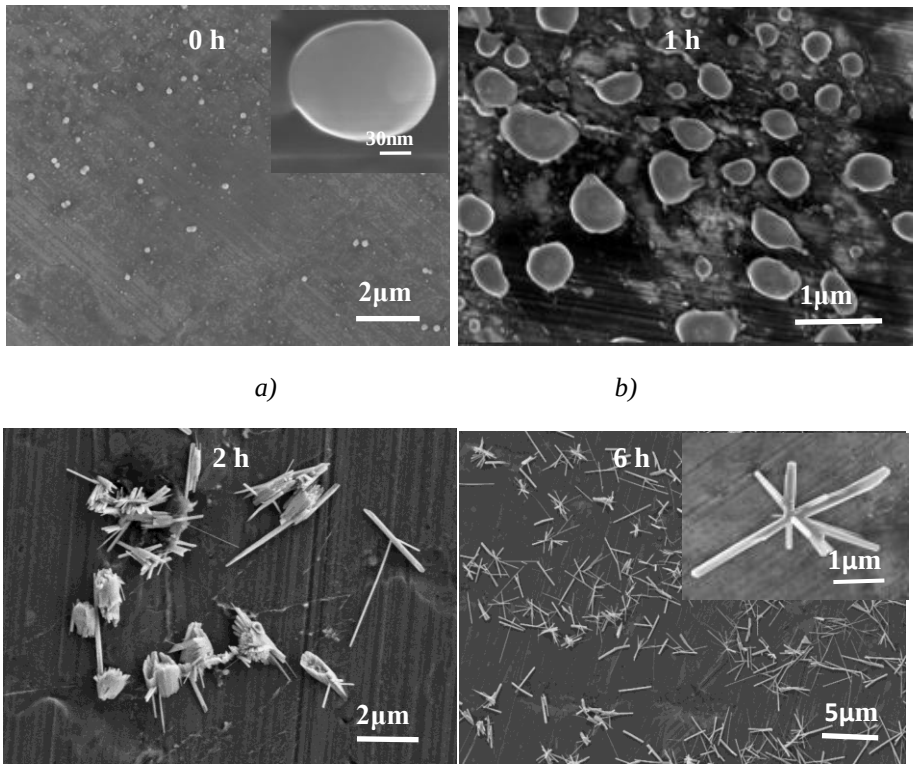

a) *b)*

c) *d)*

Fig. 4. SEM images of the as-prepared Se colloids kept at 100 ℃; for different times; (a) 0h; (b) 1 h; (c) 2h, and (d) 6h.

3.3.3 The formation mechanism of t-Se nanowires

Based on the above results, the formation mechanism of t-Se nanowires could be schematically presented in Fig. 5. According to the Stranski's rule [14], in a realistic crystal growth system, the most unstable and soluble phase were favored kinetically, thus it usually precipitated first; and then this meta stable phase can transform into a more thermodynamically stable phase [18]. According to this rule, in Se system, the unstable a-Se was firstly formed in the

solution at room temperature, and then aggregated and formed spherical a-Se colloids (step A) due to their high surface energy.

With reaction time prolonged, spherical a-Se colloids partially dissolved in the solution and lots of free selenium atoms appeared in the solution. As the concentration of free selenium atoms increased constantly, t-Se seeds (step B) gradually formed in the solution. The t-Se seeds initially grew into t-Se nanowires by consuming a number of a-Se colloids that were clustered around t-Se seeds (step C). The possible growth process for t-Se nanowires in the liquid phase was basically agreement with what Gates B[19] proposed.

In fact, the phase transformation energy from amorphous selenium to trigonal selenium is only 6.63 kJ/mol. Hence, a slightly increase in temperature will lead to the phase conversion [20]. In the solid to solid transition process of Se colloids to Se nanowires, t-Se seeds began to appear at the surface of Se colloids at high temperature (step D), as phase transformation occurred at the surface of spherical a-Se colloids firstly. With the aging time prolonged, t-Se seeds grew into t-Se nanowires (step E) together with the consuming of spherical a-Se colloids. The growth process of the t-Se nanowires was basically same as what Jian hua Zhang [17] described, but the difference was that this experiment was carried out in the solid phase, while the growth process he mentioned was carried out in the liquid phase.

In conclusion, the extended spiral chains of selenium atoms in the trigonal phase provided a natural template to define and guide the growth direction. The transition of a-Se to t-Se nanowire can not only happen in a solid-solution-solid process which coincided with the "solid-solution-solid" growth mechanism mentioned by Xie [21] et al, but also can happen in a solid to solid process as presented in this paper.

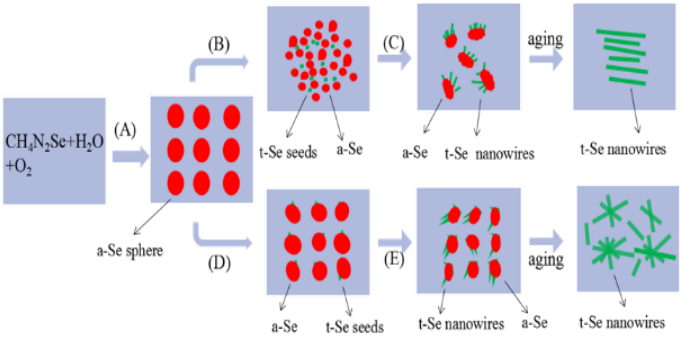

Fig. 5. Schematic map of the formation mechanism of t-Se nanowires.

4. Conclusions

The t-Se nanowires, with a diameter about 70 nm and length up to several tens of micrometers, could be obtained by in water at room temperature. The results of HRTEM, XRD, Raman and EDS showed that the t-Se nanowires obtained, with only elemental selenium, mainly grew along the [0 0 1] direction. Time-dependent experiments showed that the transition of a-Se to t-Se nanowire can not only happen in a solid-solution-solid process which coincided with the "solid-solution-solid" growth mechanism, but also can happen in a solid to solid process.

Acknowledgments

This work was supported by the National Key Research and Development Program of China (2017YFA0303403) and the National Natural Science Foundation of China (Grant No. 61974042).

References

[1] L. M. Moreau, M. R Jones, E. W. Roth, J. Wu, S. Kewalramani, M. N. O. Brien, B. R. Chen, C. A. Mirkin, M. J. Bedzyk, J. Nanoscale **11**(24), 11744 (2019).
[2] S. Kumar, J. Exp. Nanosci. **4**(4), 341 (2009).
[3] A. Malhotra, M. Maldovan, J. Heat Mass Transf. **130**, 368 (2019).
[4] S. Panchal, R. P. Chauhan, Phys. Lett. A **381**(32), 2636 (2017).
[5] N. Kumar, R. Kumar, S. Kumar, S. K. Chakarvarti, J. Mater. Sci.-Mater. Electron **25**(8), 3537 (2014).
[6] H. Chen, D. W. Shin, J. G. Nam, K. W. Kwon, J. B. Yoo, Mater. Res. Bull **45**(6), 699 (2010).
[7] D. F. Pratama, B. H. Susanto, E. Ramayeni, Iop Conference **105**, 012056 (2018).
[8] K. Zeng, S. G. Chen, Y. D. Song, H. B. Li, F. J. Li, P. Liu. Particuology **11**(5), 614 (2013).
[9] L. Zhang, Y. H. Ni, J. M. Hong, J. Phys. Chem. Solids **70**(11), 1408 (2009).
[10] B. Gates, B. Mayers, A. Grossman, Y. N. Xia, Adv. Mater **14**(23), 1749 (2002).
[11] R. A. Bley, S. M. Kauzlarich, J. Journal of the American Chemical Society **118**(49), 12461 (1996).
[12] X. Y. Gao, T. Gao, L. D. Zhang, J. Mater. Chem **13**, 6 (2003).
[13] B. T. Mayers, K. Liu, D. Sunderland, Y. N. Xia. Chem. Mat **15**(20), 3852 (2003).
[14] X. M. Li, Y. Li, S. Q. Li, W. W. Zhou, H. B. Chu, W. Chen, I. L. Li, Z. K. Tang. Cryst. Growth Des. **5**(3), 911 (2005).
[15] Y. J. Zhu, X. L. Hu. Mater. Lett. **58**(7-8), 1234 (2004).
[16] M. Steichen, P. Dale. Electrochem. Commun **13**(8), 865 (2011).
[17] J. H. Zhang, Q. S. Fu, Z. X. Cui, Y.Q. Xue. Crystengcomm **21**(3), 430 (2019).
[18] J. P. Jolivet, M. Henry, J. Livage, Metal oxide chemistry and synthesis from solution to solid state, John Wiley & Sons, French, 2000.
[19] B. Gates, B. Mayers, B. Cattle, Y. N. Xia. Adv. Funct. Mater. **12**(3), 219 (2002).
[20] L. P. Liu, Q. Peng, Y. D. Li. Nano Res **1**(5), 403 (2008).
[21] Q. Xie, Z. Dai, W. W. Huang, W. Zhang, D. K. Ma, X. K. Hu, Y. T. Qian, J. Cryst. Growth Des. **6**(6), 1514 (2006).